Electronic supplementary information

Architecturally Simple Organic Photodiodes with Highly Competitive Figures of Merit via Facile Self-Assembly Strategy

Hrisheekesh Thachoth Chandran [a,#], Hua Tang [a,b,#], Taili Liu [c,d], Sudhi Mahadevan [e], Kuan Liu [a], Zhen Lu [a], Jiaming Huang [a], Zhiwei Ren [a], Fuyou Liao [f], Yang Chai [f], Patrick WK Fong [a], Sai-Wing Tsang [e], Shirong Lu [b], Gang Li [a,*]

[a]*Department of Electronic and Information Engineering, Research Institute for Smart Energy (RISE), The Hong Kong Polytechnic University, Hung Hom, Kowloon, Hong Kong SAR, P. R. China.*

[b]*Thin-film Solar Technology Research Center, Chongqing Institute of Green and Intelligent Technology, Chinese Academy of Sciences, Chongqing, 400714, P. R. China.*

[c]*College of Physics and Electronic Information, Yunnan Normal University, Yunnan Kunming 650500, China.*

[d]*Yunnan Provincial Key Laboratory for Photoelectric Information Technology, Yunnan Normal University, Yunnan Kunming 650500, China*

[e]*Department of Materials Science and Engineering, Center of Super-Diamond and Advanced Films (COSDAF), City University of Hong Kong, Hong Kong SAR, P. R. China.*

[f]*Department of Applied Physics, The Hong Kong Polytechnic University, Hung Hom, Kowloon, Hong Kong SAR, P. R. China.*

#These authors contributed equally to this work

Email: gang.w.li@polyu.edu.hk

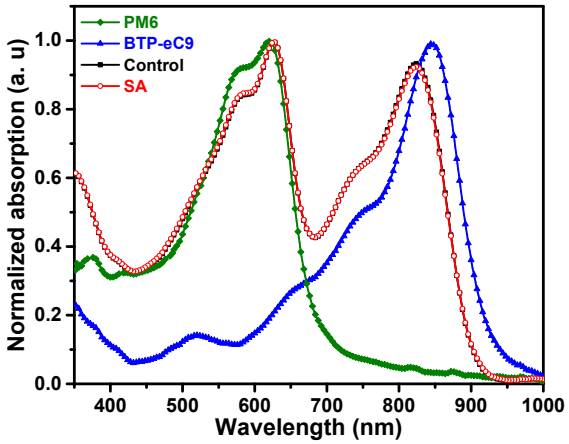

Fig. S1 Normalized absorption spectra of pristine materials (PM6 and BTP-eC9) and BHJ blends ('control' and 'SA').

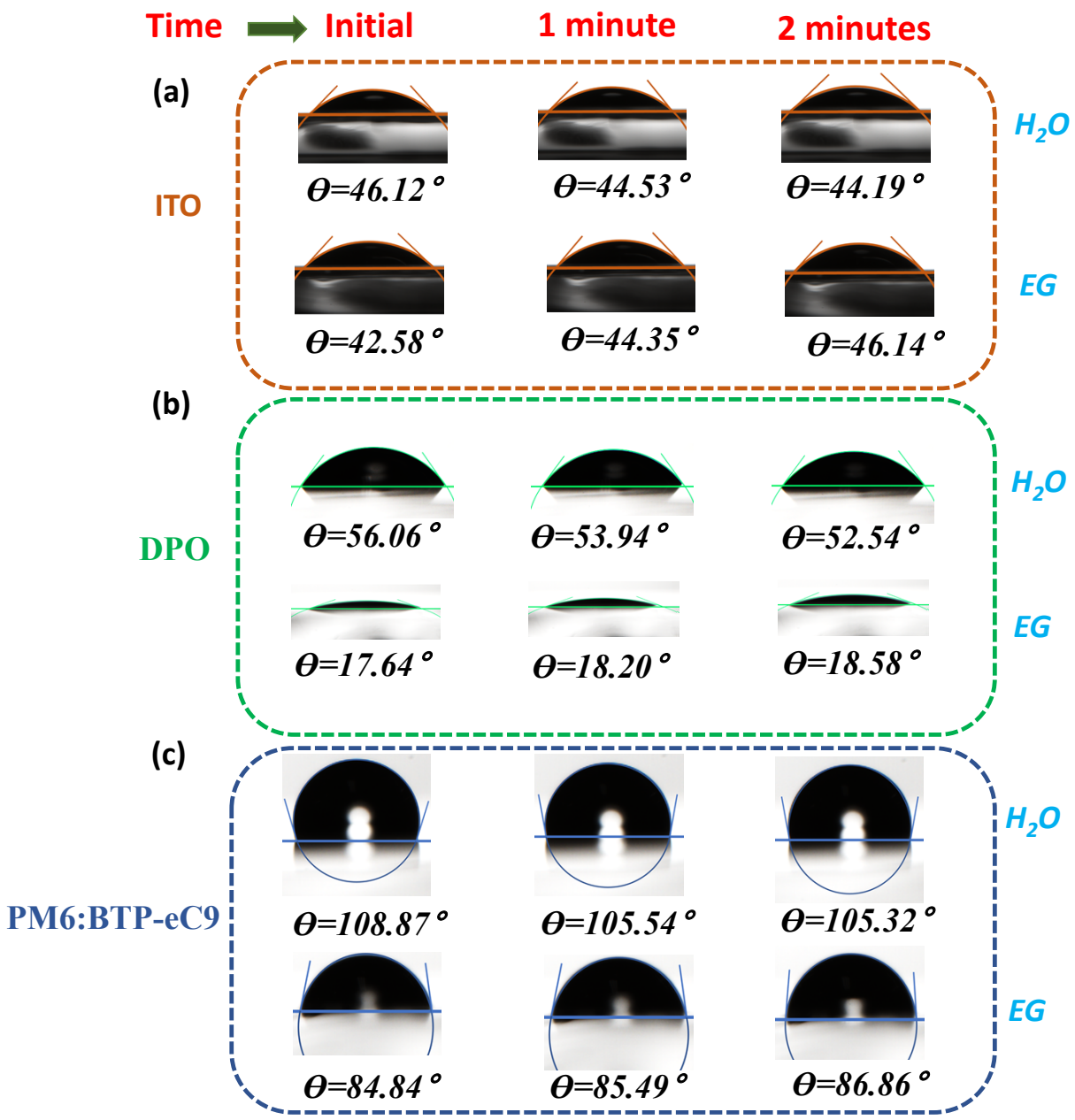

Fig. S2 The time dependent contact angles of H_2O and EG on neat (a) ITO, (b) DPO and (c) PM6:BTP-eC9 blend films.

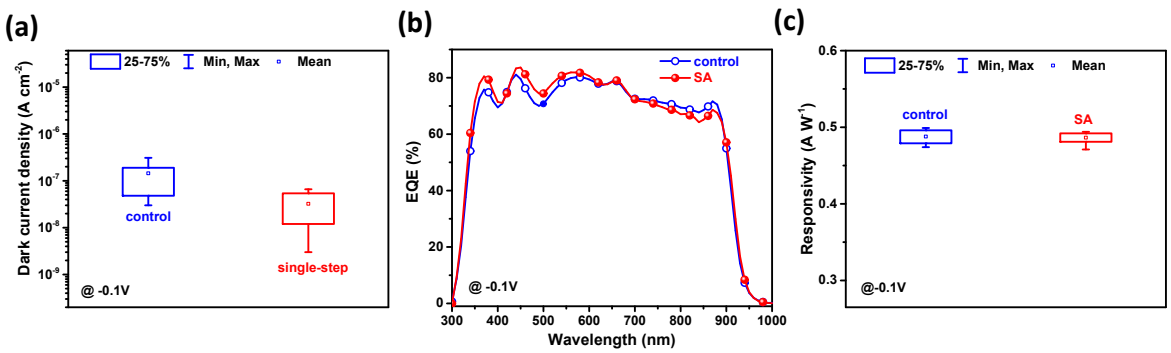

Fig. S3 (a) Statistical analysis of dark current density at -0.1V (b) EQE spectra and (c) statistical analysis of responsivity at -0.1V of 'control' and 'SA' devices

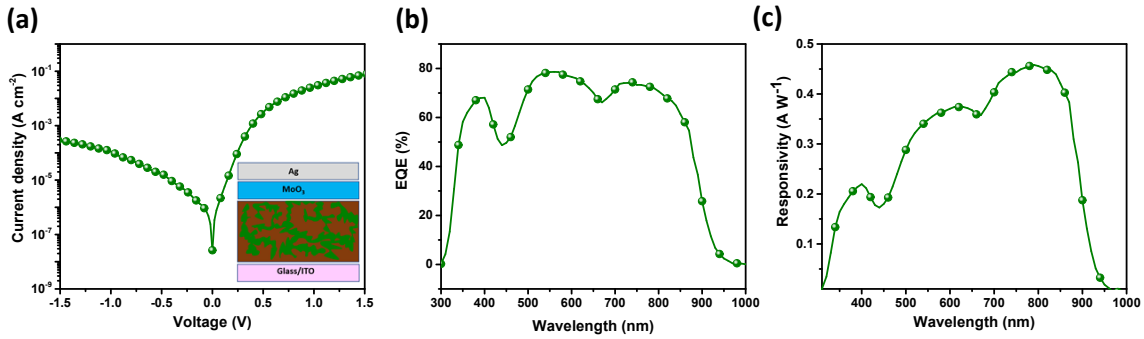

Fig. S4 (a) Dark *J-V* characteristics, (b) EQE and (c) responsivity of 'No HBL' device.

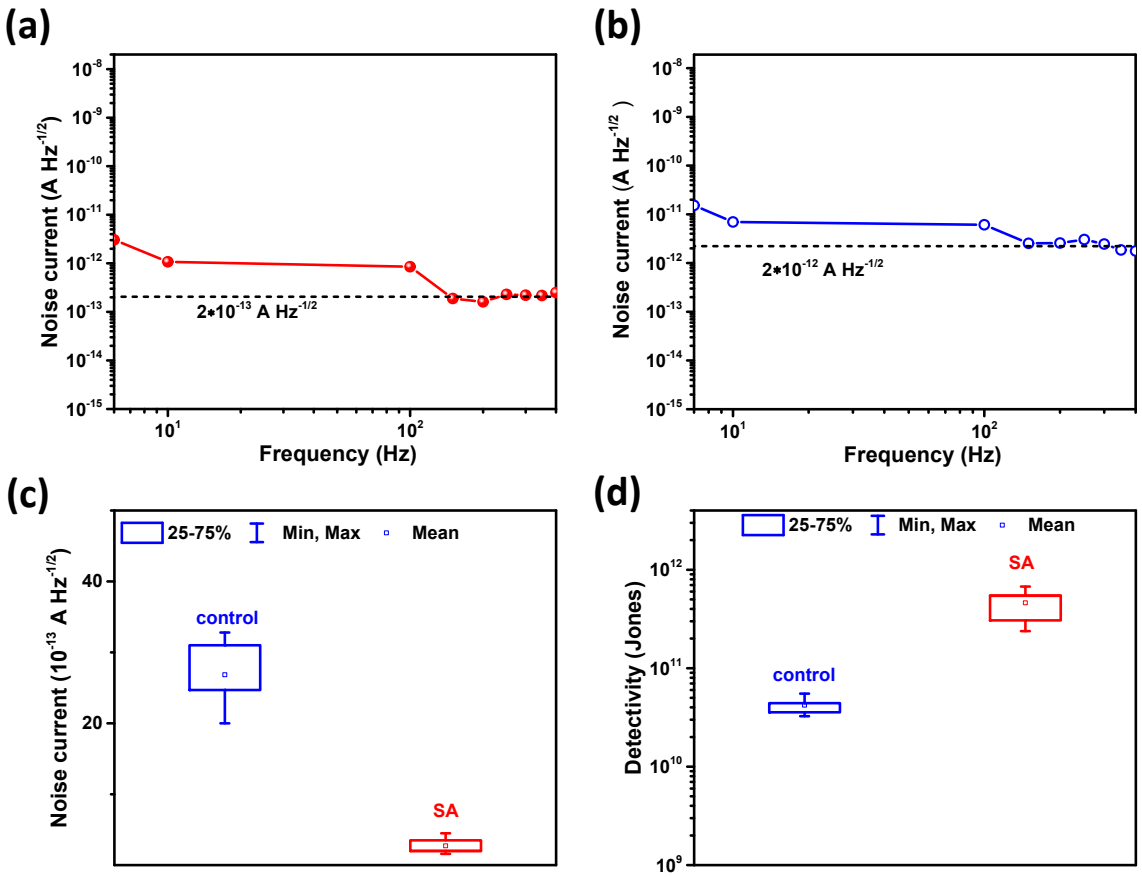

Fig. S5 Noise current-frequency plot of (a) 'SA' and (b) 'control' devices measured at -0.1V bias. Statistical analysis (N=5) of (c) noise current and (d) detectivity of 'control' and 'SA' devices

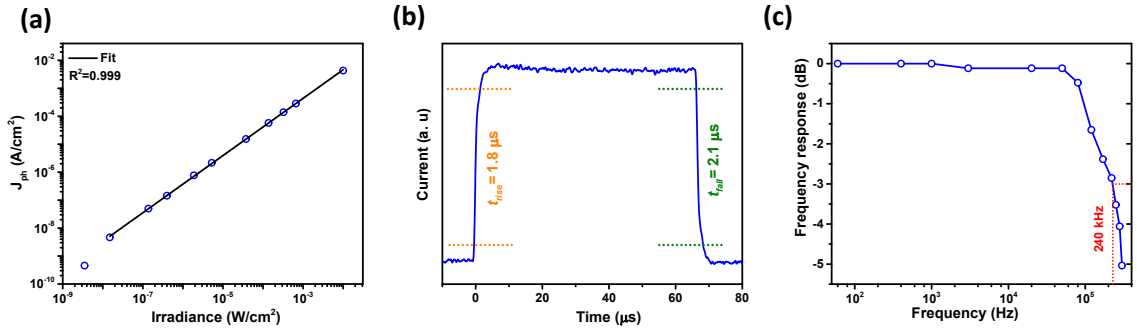

Figure S6. (a) LDR, (b) rise/fall times and (c) -3dB frequency of 'control' devices.

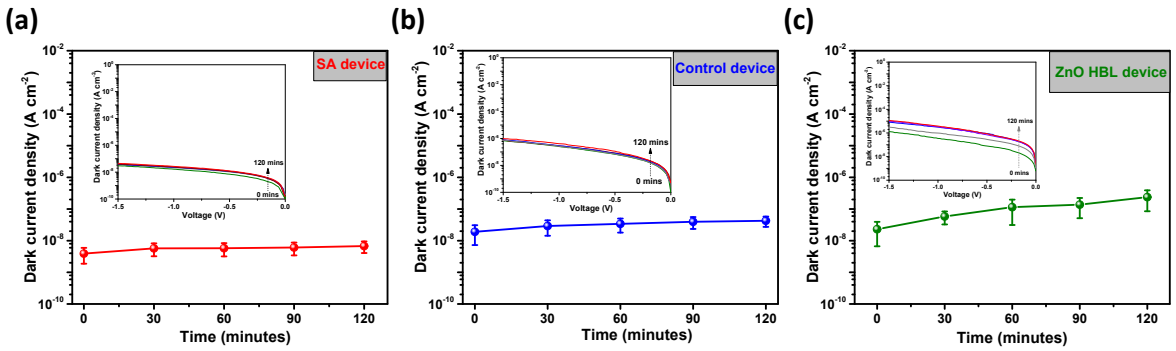

Fig. S7 The statistical analysis of photodiode stability to illumination history (in terms of dark current density at -0.1V bias) for (a) 'SA', (b) 'control' and (c) 'ZnO HBL' devices. Inset is the *J-V* curve of respective devices.

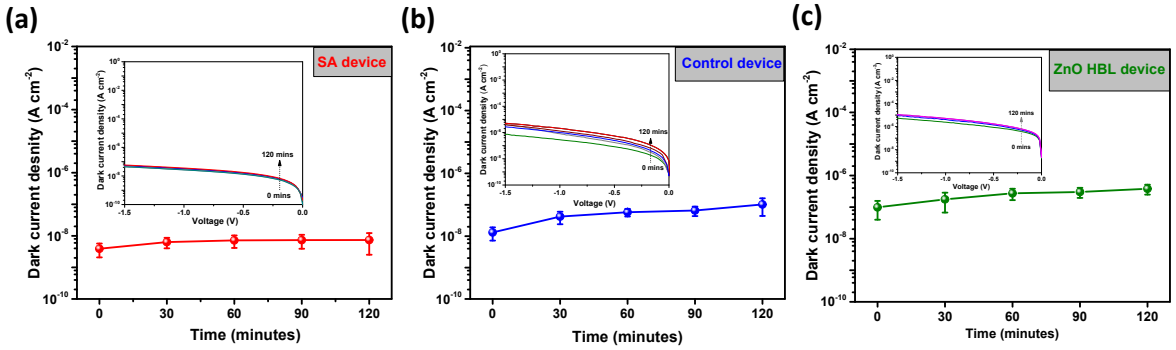

Fig. S8 Statistical analysis of heat stability in terms of dark current at -0.1 V bias for (a) 'SA', (b) 'control' and (c) 'ZnO HBL' based OPD devices. Inset is the J-V curve of respective devices.

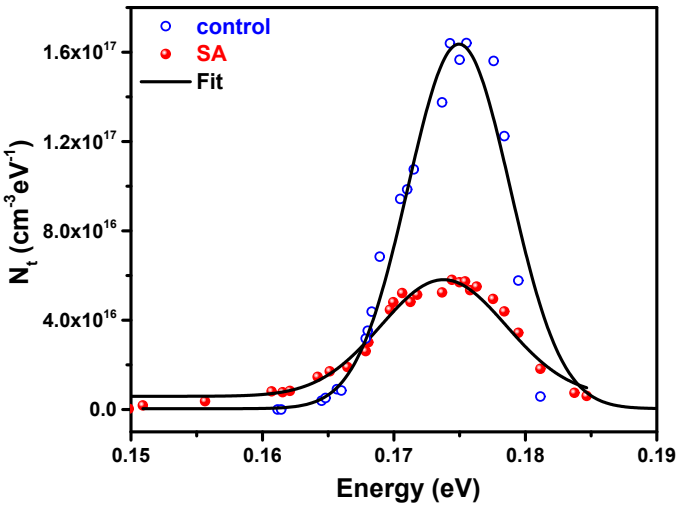

Fig. S9 N_t distribution as a function of defect energy level for the 'control' (open symbol) and 'SA' (solid symbol) devices

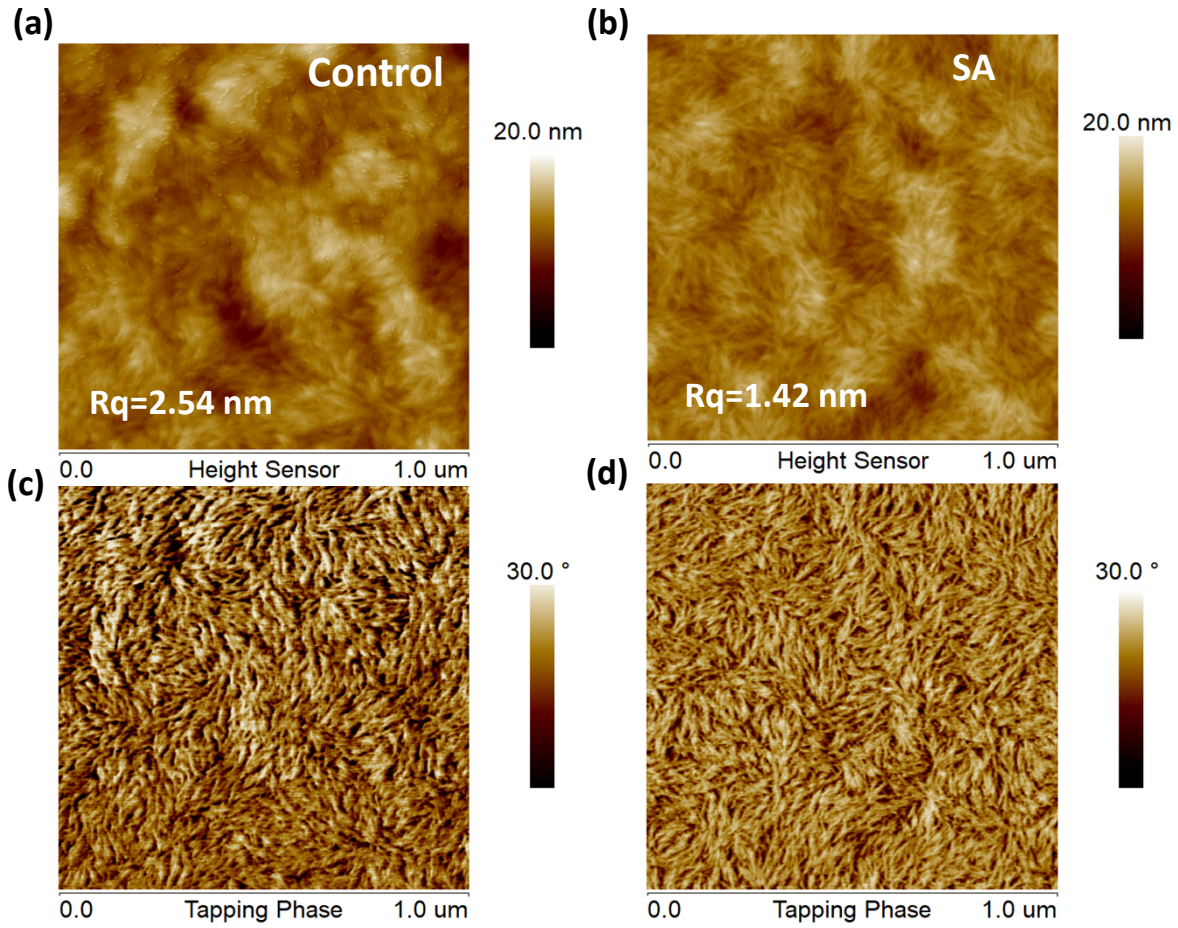

Fig. S10 AFM height images of (a) 'control' and (b) 'SA' active layer films. AFM phase images of (c) 'control' and (d) 'SA' active layer films.

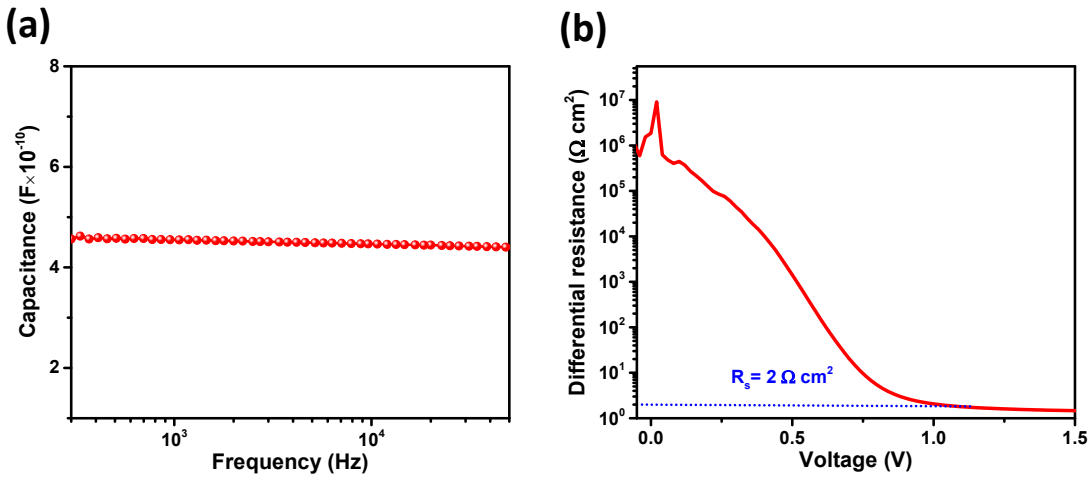

Fig. S11 (a) Capacitance-frequency and (b) differential resistance-voltage plot of 'SA' device

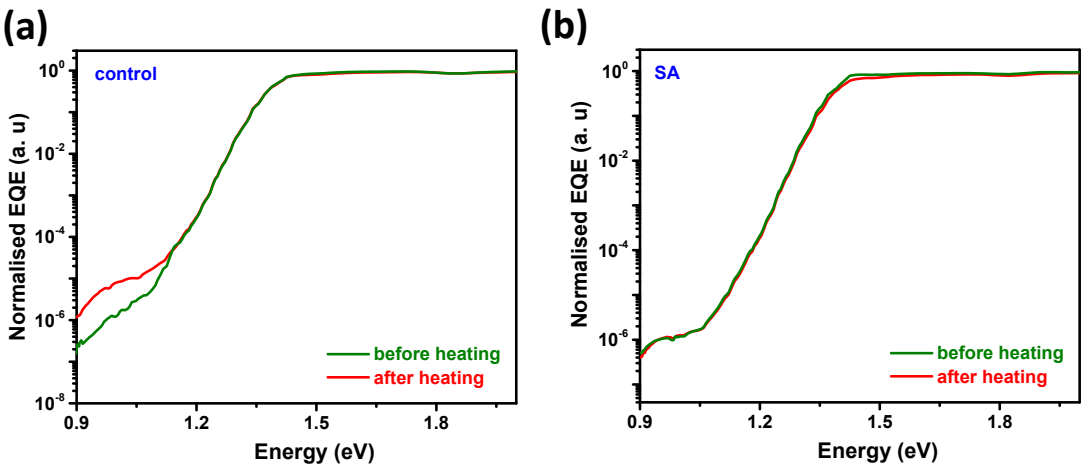

Fig. S12 Sub-bandgap EQE spectra of (a) 'control' device and (b) 'SA' device before/after heating at 100 °C.

Table S1- Contact angles and surface energy parameters of ITO, DPO, and BHJ.

Films	Contact Angle (deg)		Average Contact Angle (deg)		Surface energy γ (mJ m^{-2})
	[a] H_2O	[b] EG	[a] H_2O	[b] EG	
ITO	46.12	42.58	46.74	42.22	58.76
	46.89	41.80			
	47.23	42.30			
DPO	56.06	17.64	55.74	17.66	46.31
	55.67	17.80			
	55.50	17.54			
PM6:BTP-eC9	108.87	84.84	108.67	84.99	19.19
	108.64	85.21			
	108.50	84.92			

a) Deionized water; [b] Ethylene Glycol.

Table S2- Performance metrics comparison of reported organic photodiodes

Material system	***R*** **(AW^{-1})**	***D**** **(Jones)**	***LDR*** **(dB)**	***-3dB*** **(kHz)**	t_{rise}/t_{fall} **(µs)**	**Ref**
PTB7-Th:CO1-4Cl	0.50	1×10^{12}	126	240	-	[1]
PTB7-Th:COTIC-4	0.42	$7.9\times 10^{13*}$	115	-	21/24	[2]
NT40/IEICO-4F	0.40	8.0×10^{11}	123	100	7.1/14.9	[3]
PM6:PDTTYM	0.48	$1.3\times10^{13*}$	134	145	5.8/8.4	[4]
P3HT:ICBA	0.3	7×10^{12}	160	15	35/-	[5]
PTQ10:O-FBR	0.34	9.6×10^{12}	71	110	12/15	[6]
PBDTTT-C-T:FOIC	0.30	2.0×10^{13}	106	30	12/15	[7]
PTB7-Th:CO1-4F	0.46	1.5×10^{12} *	-	-	-	[8]
D18/Y6	0.50	2.5×10^{11}	83	-	15/14	[9]
PM6:BTP-eC9	0.50	7.1×10^{11}	140	300	1.4/1.6	This work

*shot noise limited detectivity

References

1. J. Huang, J. Lee, J. Vollbrecht, V. V. Brus, A. L. Dixon, D. X. Cao, Z. Zhu, Z. Du, H. Wang and K. Cho, *Adv. Mater.*, 2020, **32**, 1906027.
2. J. Simões, T. Dong and Z. Yang, *Adv. Mater. Interfaces*, 2022, **9**, 2101897.
3. Z. Huang, Z. Zhong, F. Peng, L. Ying, G. Yu, F. Huang and Y. Cao, *ACS Appl. Mater. Interfaces*, 2020, **13**, 1027-1034.
4. Y. Zheng, Y. Chen, Y. Cao, F. Huang, Y. Guo and X. Zhu, *ACS Materials Letters*, 2022, **4**, 882-890.
5. C. Fuentes-Hernandez, W.-F. Chou, T. M. Khan, L. Diniz, J. Lukens, F. A. Larrain, V. A. Rodriguez-Toro and B. Kippelen, *Science*, 2020, **370**, 698-701.
6. H. Bristow, P. Jacoutot, A. D. Scaccabarozzi, M. Babics, M. Moser, A. Wadsworth, T. D. Anthopoulos, A. Bakulin, I. McCulloch and N. Gasparini, *ACS Appl. Mater. Interfaces*, 2020, **12**, 48836-48844.
7. G. Liu, T. Li, X. Zhan, H. Wu and Y. Cao, *ACS Appl. Mater. Interfaces*, 2020, **12**, 17769-17775.
8. J. Lee, S.-J. Ko, H. Lee, J. Huang, Z. Zhu, M. Seifrid, J. Vollbrecht, V. V. Brus, A. Karki and H. Wang, *ACS Energy Lett.*, 2019, **4**, 1401-1409.
9. Y. Wei, H. Chen, T. Liu, S. Wang, Y. Jiang, Y. Song, J. Zhang, X. Zhang, G. Lu and F. Huang, *Adv. Funct. Mater.*, 2021, **31**, 2106326.